




# Temporal Correlation between Positive-Charged Cosmic Ray Flux and Solar Magnetic Field Variation: Insights from Delayed Modulation Analysis

SHAOKUN GONG <sup>1</sup>, LINJING DUAN,<sup>1</sup> JIAWEI ZHAO,<sup>1</sup> XUEYU WEI,<sup>1</sup> JIE FENG <sup>1</sup> AND ZHIBING LI <sup>1</sup>

<sup>1</sup> School of Science, Shenzhen Campus of Sun Yat-sen University, Shenzhen 518107, China

## ABSTRACT

We present an analysis of the time-dependent modulation of galactic cosmic rays near Earth, with a focus on the cosmic proton flux and solar magnetic field strength. Using data from the Alpha Magnetic Spectrometer (AMS) and the Wilcox Solar Observatory, we identify a significant time-lagged relationship between the observation of two missions. Our model incorporates a weighted magnetic field parameter to address the hemispheric asymmetry in solar magnetic fields and captures the temporal evolution of cosmic-ray proton spectra in relation to solar activity. We find a time lag of approximately 10 months, varying with cosmic ray rigidity. At 1 GV, the time lag is 360 days, while it is 300 days above 3 GV. This offers predictive insights into cosmic ray modulation within the heliosphere. These results enhance the accuracy of space weather forecasting models, with significant implications for the safety of space missions and aviation.

*Keywords:* cosmic proton flux — solar magnetic field— solar modulation — time lag

## 1. INTRODUCTION

In recent years, the precision of cosmic-ray (CR) detection experiments has significantly improved, measuring temporal variations in cosmic rays increasingly important. These variations provide crucial insights into the dynamic processes within the heliosphere. Solar activities, such as solar wind, sunspot numbers, changes in the solar magnetic field, and solar modulation effects, significantly impact the energy spectra of CR. Therefore, studying these changes is essential for understanding CR propagation in the heliosphere.

The necessity of measuring temporal variations in low-energy cosmic rays lies in their correlation with the solar activity cycle, particularly the quasi-periodic 11-year solar cycle, which affects the flux and energy distribution of cosmic rays reaching the Earth. Observationally, the relationship between solar activity and cosmic-ray flux intensity has been widely validated. This relationship underscores the importance of continuous and precise CR measurements to understand the underlying physical mechanisms.

Globally, several experiments and missions have contributed to this field by providing extensive data on cosmic rays. For instance, Voyager 1 ([Webber 2018](#); [Provornikova et al. 2014](#)) was the first to measure cosmic rays in interstellar space, while long-term missions like PAMELA ([Martucci et al. 2018](#); [Adriani et al. 2013](#)) and AMS ([Aguilar et al. 2021a](#)) have been continuously monitoring cosmic rays. These missions have significantly enriched our understanding by offering time-resolved data on cosmic-ray particles and antiparticles. Ground-based observations also play a vital role, with neutron monitors and other detectors providing continuous data that complement space-based observations. The comprehensive datasets collected by these observatories have enabled the development of detailed models of CR propagation and solar modulation ([Potgieter 2014a](#)), enhancing our understanding of heliospheric processes ([Ferreira & Potgieter 2004](#)).

Time-dependent structures in the energy spectra of galactic cosmic rays (GCRs) are expected to arise due to solar modulation once they enter the heliosphere. Solar modulation involves several processes, including convection, diffusion, particle drift, and adiabatic energy changes. This complex interplay of processes alters the energy spectra of GCRs as they propagate through the heliosphere, highlighting the significance of studying solar modulation to understand the variations in cosmic

ray fluxes (Tomassetti 2015; Tomassetti & Donato 2015; Feng et al. 2016).

In this letter, utilizing an extensive dataset of modulated and interstellar cosmic-ray measurements collected from the Alpha Magnetic Spectrometer, we have discovered a significant correlation between solar activity, particularly the solar magnetic field, and the cosmic rays. This correlation can aid in the development of predictive models for cosmic ray modulation. Our approach incorporates a "delayed" relationship to capture the impact of solar activity observations and the conditions within the modulation region, estimating a time lag  $\Delta T$  of approximately one year. Previous empirical studies have highlighted the significance of this lag in cosmic-ray modulation models (Tomassetti et al. 2017a). We will illustrate that recent direct measurements of cosmic rays indicate a lag of about ten months relative to solar magnetic activity. This finding establishes the timescale for the evolving conditions in the heliosphere, allowing us to predict near-Earth cosmic-ray fluxes with considerable lead time.

Our findings are crucial for the development of models to predict space weather effects, which are becoming a significant concern for both space missions and air travelers. These results not only contribute to scientific knowledge in plasma and solar astrophysics but also address practical issues related to the safety and reliability of space and aviation operations.

This letter is organized as the following. The analytical approach to the correlation between the solar magnetic field strength and the proton fluxes is presented in Section 2. The delayed effect of the solar magnetic field strength on the proton flux is presented in Section 3. We summarize our study in Section 4.

## 2. METHODOLOGY

Numerous studies have established that the solar magnetic field significantly influences the heliospheric magnetic field (HMF), thereby affecting the modulation of CRs entering the heliosphere. The HMF modulates CRs through various processes (Usoskin et al. 2005; Potgieter 2013), including drift, diffusion, convection, and adiabatic energy loss, altering their energy spectra and spatial distribution (Ferreira & Potgieter 2004; Cliver et al. 1998).

Putri et al. (2024) indicates an asymmetry in the magnetic fields of the northern and southern solar poles, which must be accounted for when modeling the impact on CR. This asymmetry can be further understood within the framework of the solar cycle's polarity. The solar cycle can be categorized into two distinct periods

based on the polarity of the solar magnetic field: positive polarity ( $A > 0$ ) and negative polarity ( $A < 0$ ).

Therefore, a simple additive approach to combining these fields is insufficient. The modulation of cosmic rays differs between these periods due to changes in the HMF structure, with the drift patterns of charged particles being significantly influenced by the direction of the HMF (Jokipii et al. 1977; Potgieter 2014b).

To address this asymmetry, we introduce a weighting parameter  $w$  to adjust the influence between the magnetic field of the northern hemisphere ( $B_N$ ) and the southern hemisphere ( $B_S$ ). The weighted magnetic field  $B_{\text{weighted}}$  is defined as:

$$B_{\text{weighted}} = \frac{B_N - wB_S}{1 + w}, \quad (1)$$

As  $w \rightarrow 0$ , the magnetic field of the northern hemisphere ( $B_N$ ) predominates. Conversely, as  $w \rightarrow \infty$ , the magnetic field of the southern hemisphere ( $B_S$ ) becomes dominant. When  $w = 1$ , the effects on the cosmic ray from both hemispheres are equal.

The solar magnetic field data utilized in this research was sourced from the publicly accessible archives of the Wilcox Solar Observatory (Scherrer et al. 1977). Data points were systematically recorded every 10 days.

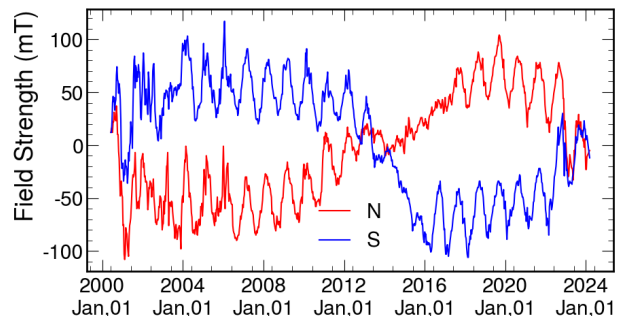


**Figure 1.** The Wilcox Solar Observatory (Scherrer et al. 1977) records the variations in the magnetic field strength at the solar north and south poles from 2000 to 2024.

During the period from 2017 to 2020, the magnetic field distribution remained relatively stable, with no significant trends. To refine our analysis and mitigate variability, we adjusted  $w$  to smooth the magnetic field data, reducing noise and non-periodic variations in cosmic ray flux. This adjustment enhances model accuracy by better capturing the modulation effects of the solar magnetic field. Notably, the proton flux during this period showed no large time structure in 10-day bins. We began with  $w = 1$ , assuming equal weighting of the northern and southern magnetic fields, followed by a linear fit and a calculation of the  $\chi^2$ .

Next, we varied the weight  $w$  within the range of 0.6 to 1.2. We re-fitted the magnetic field data with a linear function for each value of  $w$  and computed the differences in  $\chi^2$  for each weight. This iterative approach allowed us to identify the optimal weighting parameter  $w$  that minimized the variability and provided the smoothest temporal distribution of the solar magnetic fields. The variance  $\chi^2$  is calculated using the following formula:

$$\chi^2(w) = \sum_i \left( \frac{y_i(w) - y_{\text{fit},i}}{y_i(w)} \right)^2, \quad (2)$$

where  $y_i(w)$  is the effective magnetic field,  $y_{\text{fit},i}$  is the value from the linear fit. From 2017 to 2020, the magnetic field distribution remained relatively stable,  $i$  loops from 2017 to 2020, including 111 data points.

To ensure consistency in our analysis of the solar magnetic field's influence on cosmic rays, we addressed the polarity reversal that occurred around 2013. Observational data and theoretical models indicate that the solar magnetic field underwent a polarity reversal during this period, switching from negative to positive polarity (Mordvinov & Yazev 2014; Pishkalo 2019; Aslam et al. 2023). We defined the post-2013 magnetic field as having a positive polarity. To maintain a consistent polarity for the entire dataset, we took the absolute value of the pre-2013 magnetic field measurements, effectively normalizing the data to a uniform polarity standard. Additionally, the weights  $w$  were set differently for the periods before and after the polarity reversal, reflecting the changes in the magnetic field's influence.

Furthermore, to align the frequency with the solar magnetic field data, we applied a weighted average to the daily proton flux data over ten days in Appendix A (Ebert et al. 2022), converting it into ten-day average flux data. Figure 1 shows that the time distribution of proton flux exhibits a very similar pattern to the time distribution of the solar magnetic field. We can define a time lag function as follows. Let  $Y$  denote the proton flux and  $X$  denote the weighted solar magnetic field strength determined by Equation 1. We introduce the following equation to model the relationship:

$$Y = aX(t + \Delta T) + b \quad (3)$$

Here,  $\Delta T$  represents the time lag between the solar activity indices and the medium properties of the modulation. This function allows us to quantify the delay between changes in solar magnetic activity and corresponding responses in cosmic ray flux. Our model is defined by three free parameters:  $a, b, \Delta T$ , which are constrained using extensive data. This data includes proton

measurements collected by the AMS experiment from 2011 May to 2019 December. Each data point  $J(t_j, E_k)$  represents the cosmic-ray flux at a specific time  $t_j$  while  $\hat{J}_{j,k}$  denotes the predicted value from the linear fit. The calculations incorporate delayed functions of the physical inputs. We utilize a global  $\chi^2$  estimator to determine the optimal time delay.

$$\chi^2(a, b, \Delta T) = \sum_{j,k} \left[ \frac{J(t_j, E_k; a, b, \Delta T) - \hat{J}_{j,k}}{\sigma_{j,k}} \right]^2, \quad (4)$$

where  $\sigma_{j,k}$  represents the experimental errors in the data. By adjusting  $\Delta T$  to find the value that minimizes  $\chi^2$ , we determine the time delay relationship between solar magnetic activity and cosmic rays,

According to theoretical references, the error range of the  $\chi^2$  distribution is determined when the  $\chi^2$  increases a certain specified value (Behnke et al. 2013; Gregory 2005). For a given set of data, the confidence region is defined by the inequality:

$$\chi^2(\theta) \leq \chi^2_{\text{min}} + \Delta\chi^2. \quad (5)$$

Here,  $\Delta\chi^2$  is typically derived from the  $\chi^2$  distribution based on the desired confidence level and the number of degrees of freedom in the model.

This ensures that the error range corresponds to the interval in which the parameter values are statistically likely to be found, with the observed data on hand.

We used proton data spanning 2000 days combined with solar magnetic field data from 2014 to 2019. The weighted average method was employed to calculate the mean flux of 10 days. To find the optimal time shift that minimizes the  $\chi^2$  value, we shifted the proton flux data backward and forward by a total of 730 days. Each shift corresponds to one data point, which is equivalent to 10 days, resulting in 73 shifts in total.

### 3. RESULTS

Firstly, we calculated the weight of the solar magnetic field. Using relatively stable data points from 2017 to 2020, 111 points, we performed a linear fit to obtain the results. Without applying any weight, the composite magnetic field had a  $\chi^2/ndf = 29.21/108$ .

In Figure B1, by using Equation 2 to find the minimum  $\chi^2/ndf$ , we achieved a value of 23.27/108, corresponding to an optimal weight of  $w = 0.78$ . By setting this weight, we smoothed the composite total solar magnetic field, thereby eliminating fluctuations irrelevant to cosmic ray modulation. The difference in chi-square values around 6 is significant, indicating a clear discrepancy.

After determining the optimal weight for the  $A > 0$  period, the global fit has been performed on 2560 proton data points collected between 2014 and 2019 (in  $A > 0$  conditions) at rigidity intervals between 1 and 33.5 GV (Aguilar et al. 2021b). The best-fit parameters for each of the 27 rigidity intervals were determined. The optimal fit parameters in the 1.00-1.16 GV interval are  $a = 19.3 \pm 0.1$ ,  $b = 349 \pm 2$ , and  $\chi^2/ndf = 3621.0/198$ , with a time delay of  $360 \pm 5$  days as determined by the confidence region 5. When the time delay was not set, the fit results were  $a = 17.2 \pm 0.1$ ,  $b = 408 \pm 3$ , and  $\chi^2/ndf = 43116.3/198$ . These results are based on the positive polarity period data from 2014 to 2019.

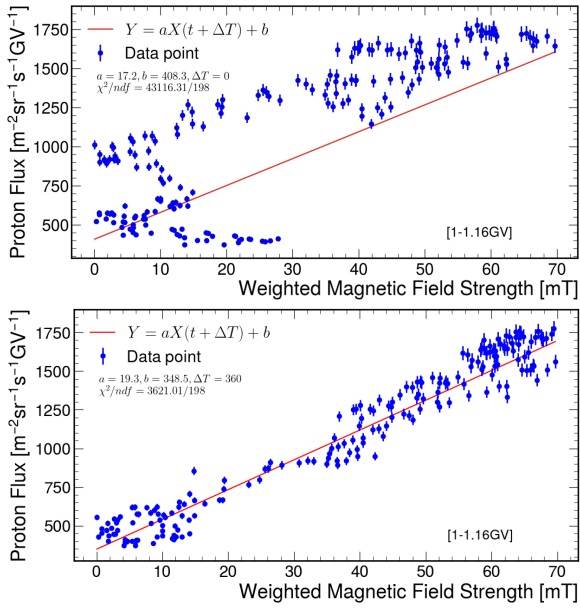


**Figure 2.** Comparison of the weighted magnetic field strength versus the proton flux in the rigidity range 1.00-1.16 GV. The top panel shows the original ( $\Delta T = 0$ ) distribution compared with a linear function ( $\chi^2/ndf = 43116.3/198$ ), while the bottom panel shows the shifted ( $\Delta T = 360$  days) distribution ( $\chi^2/ndf = 3621.0/198$ ).

In Figure 2, the optimal time lag adjustment results in a significantly better fit to the data, reducing the  $\chi^2$  value from 43116 to 3621. This substantial reduction in  $\chi^2$  value indicates that the time lag plays a crucial role in accurately modeling the relationship between the solar magnetic field and cosmic ray proton flux, resulting in a better linear relationship.

Figure 3 further supports this finding by showing the time series comparison between the weighted solar magnetic field strength and cosmic ray proton flux. The top panel presents the relationship without accounting for the time lag, while the bottom panel displays the relationship with the optimal time lag applied. The blue

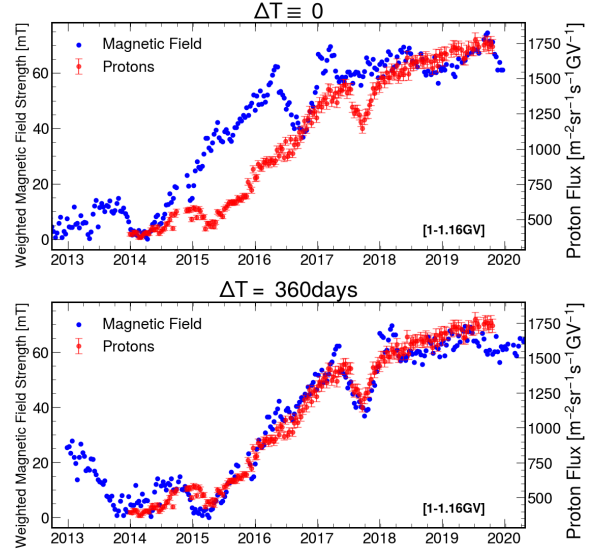


**Figure 3.** Comparison of cosmic ray proton flux and weighted solar magnetic field strength for rigidity 1.00-1.16 GV. The blue points represent the solar magnetic field strength, and the red points represent the flux of protons. The top panel shows the magnetic field strength and the proton fluxes do not vary simultaneously, while the bottom panel shows that they vary in the same trend if a delay of 360 days is applied to the magnetic field.

points represent the solar magnetic field strength, and the red points represent the flux of protons. With the optimal time lag, the alignment between the variations in the magnetic field and proton flux is significantly improved.

We performed multiple calculations in different rigidity intervals and observed a trend where the time delay decreases with increasing rigidity. This effect is more pronounced in the 1-5 GV interval. As rigidity increases, the time delay tends to stabilize. However, due to the increasing measurement errors of AMS with higher rigidity, the errors defined by the confidence region in Equation 5 also increase. Specifically, in the 1.00-1.16 GV rigidity interval, the optimal time delay is  $360^{+40}_{-2}$  days. In the 13-16.6 GV interval, the optimal delay is  $300^{+272}_{-141}$  days.

In this study, we focused on the time delay relationship between cosmic rays and the solar magnetic field during the  $A > 0$  period (2014-2020). Our calculations indicate a time delay ranging from 360 days to 300 days, depending on rigidity. At rigidity levels above 22.8 GV, the time lag is no longer significant. During the solar magnetic field reversal period (Owens & Forsyth 2013), the constantly changing polarity makes it challenging to establish a fixed time delay pattern to explain the discrepancies between cosmic rays and the solar magnetic field (Zerbo et al. 2013; McComas et al. 2000).



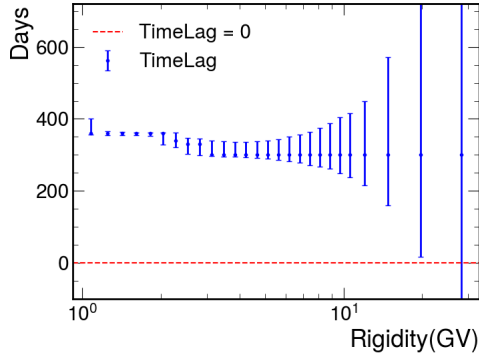


**Figure 4.** Rigidity dependence of the time lag. It includes the error determined using Equation 5. The points indicate the time delay length where  $\chi^2$  is minimized. The red dash line along 0 is to guide your eye.

Figure 5 shows the weighted magnetic field strength and the flux of cosmic rays (protons and positrons) over time from 2011 to 2022. The fluxes of protons and positrons are displayed on the right axis in red and green, respectively. The shaded region marks the period of the solar magnetic field reversal, where the polarity change complicates the identification of a consistent time delay between cosmic ray flux and magnetic field variations. From our study, we observed that during the  $A > 0$  period (2014-2020), there is a notable time delay in the response of cosmic ray flux to changes in the solar magnetic field, which varies with rigidity. In contrast, during the  $A < 0$  period, no similar time delay was observed, suggesting different modulation effects under positive and negative polarity cycles.

For the  $A < 0$  period, since AMS data collection started in 2011, we can only discuss cosmic ray flux variations from 2011 to 2014. Della Torre et al. (2012) noticed that the modulation effect during the negative polarity period on negatively charged particles may be similar to the modulation effect on positively charged particles during the positive polarity period with the positron fraction data provided by AMS-01 and PAMELA.

Therefore, we also examined the delay relationship between electrons (Aguilar et al. 2023) and the solar magnetic field from 2011 to 2014, finding a similar time delay of  $390^{+56}_{-7}$  days for electrons in the rigidity range of 1-1.71 GV as is shown in Figure B2. However, due to the later start of AMS data collection and the insufficient amount of data, we cannot provide a conclusive and accurate result. Future calculations can leverage the new data currently being measured by AMS (Aguilar et al. 2021a) for the next solar cycle. Crucial tests can be performed by AMS through detailed measurements of individual particle fluxes for  $p$ ,  $\bar{p}$ ,  $e^+$ , and  $e^-$ . Such measurements, under varying polarity conditions and during

polarity reversals, can offer deeper insights into the dynamics of cosmic ray modulation and the effects of the solar magnetic field on cosmic rays.

We have found that the solar magnetic field exhibits a delayed effect, and other literature suggests that the sunspot number also experiences a delay (Tomassetti et al. 2017b). Additionally, various other solar parameters can be considered. In the future, we can apply machine learning methods to incorporate these different parameters to predict cosmic ray behavior more effectively.

#### 4. CONCLUSION

In this letter, we find the correlations between the positive cosmic ray fluxes and the solar magnetic field data from the North and South hemispheres. Our analysis primarily focuses on the 24th solar cycle post-2013, corresponding to the  $A > 0$  positive polarity period. We defined a parameter  $w = 0.78$  to adjust the weights of

the N and S hemispheres to best describe the magnetic fields affecting cosmic rays. We calculated the time delay of cosmic rays using the weighted average magnetic field. Our model successfully predicted the temporal evolution of cosmic-ray proton spectra in the 24th solar cycle after the solar magnetic field reversal as measured by the AMS experiment. Once the correlation between modulation parameters and solar activity indices is established, our model demonstrates high predictive accuracy. By utilizing extensive cosmic-ray proton data, our research uncovered a significant aspect of cosmic-ray modulation dynamics within the expanding heliosphere. Specifically, we identified a time lag  $\Delta T$  of approximately 10 months between cosmic-ray data in the 1-33.5 GV range and solar magnetic field data, contingent on the heliospheric conditions.

A noteworthy outcome of our findings is the ability to predict the galactic cosmic-ray flux at Earth using solar activity indices observed at the time  $t - \Delta T$ . This capability is crucial for real-time space weather forecasting, an important consideration for human spaceflight.

In this work, the parameter  $\Delta T$  was determined by correlating AMS measurements of cosmic-ray protons from 2014 to 2019 with solar magnetic field data sampled every 10 days. Future research could include the use of neutron monitor data (Smith & Doe 2022; Maurin et al. 2015), longer observation periods, or accounting for periodicities and latitudinal dependencies in solar magnetic field measurements (Potgieter 1997). Due to the current precision of available solar magnetic field data, we could not test these additional hypotheses. However, a detailed re-analysis of our model will be possible with

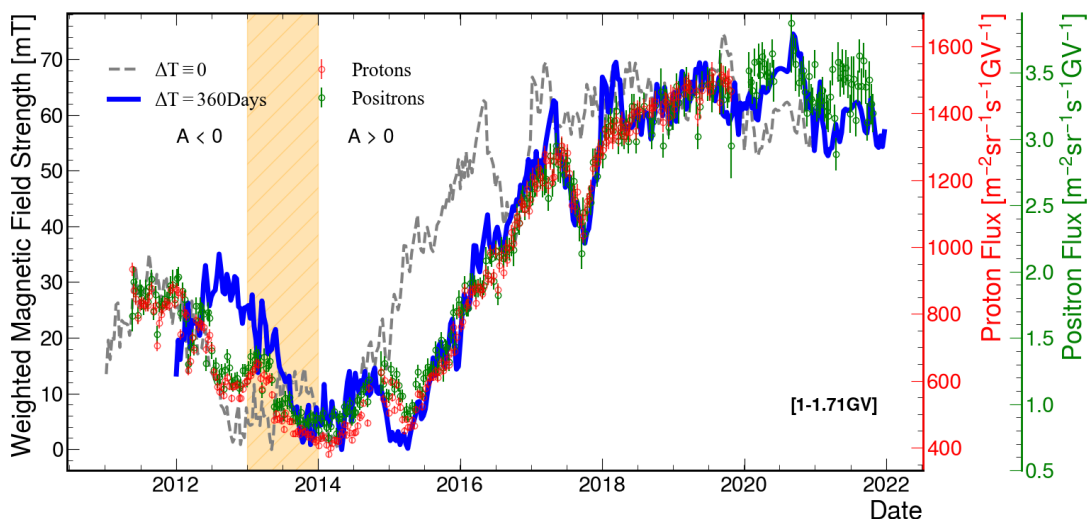


**Figure 5.** Time profile of the proton flux at Rigidity=1-1.71GV. Best-fit calculations are shown as a thick blue solid line, in comparison with the data (Aguilar et al. 2021b). Calculations for  $\Delta T \equiv 0$  are shown as thin dashed lines. The orange shaded bars indicate the magnetic reversals of the Sun’s polarity at 2013 (Sun et al. 2015).

the forthcoming monthly resolved data from AMS on cosmic-ray particle and antiparticle fluxes.

The results of this study provide significant insights into the dynamics of cosmic-ray modulation and offer practical implications for space weather prediction, enhancing the safety and planning of human space missions.

This work is supported in part by the Fundamental Research Funds for the Central Universities, and the Sun Yat-sen University Science Foundation.

## REFERENCES

- Adriani, O., Barbarino, G. C., Bazilevskaya, G. A., et al. 2013, *The Astrophysical Journal*, 765, 91, doi: [10.1088/0004-637X/765/2/91](https://doi.org/10.1088/0004-637X/765/2/91)
- Aguilar, M., Ali Cavasonza, L., Ambrosi, G., et al. 2021a, *Physics Reports*, 894, 1, doi: <https://doi.org/10.1016/j.physrep.2020.09.003>
- Aguilar, M., Cavasonza, L. A., Ambrosi, G., et al. 2021b, *Phys. Rev. Lett.*, 127, 271102, doi: [10.1103/PhysRevLett.127.271102](https://doi.org/10.1103/PhysRevLett.127.271102)
- . 2023, *Phys. Rev. Lett.*, 130, 161001, doi: [10.1103/PhysRevLett.130.161001](https://doi.org/10.1103/PhysRevLett.130.161001)
- Aslam, O. P. M., Luo, X., Potgieter, M. S., Ngobeni, M. D., & Song, X. 2023, *The Astrophysical Journal*, 947, 72, doi: [10.3847/1538-4357/acc24a](https://doi.org/10.3847/1538-4357/acc24a)
- Behnke, O., et al., eds. 2013, *Data analysis in high energy physics* (Weinheim, Germany: Wiley-VCH). <http://www.wiley-vch.de/publish/dt/books/ISBN3-527-41058-9>
- Cliver, E. W., Boriakoff, V., & Feynman, J. 1998, *Geophysical Research Letters*, 25, 1035, doi: <https://doi.org/10.1029/98GL00499>
- Della Torre, S., Bobik, P., Boschini, M. J., et al. 2012, *Advances in Space Research*, 49, 1587, doi: <https://doi.org/10.1016/j.asr.2012.02.017>
- Ebert, P. L., Gessert, D., & Weigel, M. 2022, *Physical Review E*, 106, 045303, doi: [10.1103/PhysRevE.106.045303](https://doi.org/10.1103/PhysRevE.106.045303)
- Feng, J., Tomassetti, N., & Oliva, A. 2016, *Phys. Rev. D*, 94, 123007, doi: [10.1103/PhysRevD.94.123007](https://doi.org/10.1103/PhysRevD.94.123007)
- Ferreira, S. E. S., & Potgieter, M. S. 2004, *ApJ*, 603, 744, doi: [10.1086/381649](https://doi.org/10.1086/381649)
- Gregory, P. 2005, *Bayesian Logical Data Analysis for the Physical Sciences: A Comparative Approach with Mathematica® Support* (Cambridge University Press)
- Jokipii, J. R., Levy, E. H., & Hubbard, W. B. 1977, *The Astrophysical Journal*, 213, 861, doi: [10.1086/155218](https://doi.org/10.1086/155218)
- Martucci, M., et al. 2018, *Astrophys. J. Lett.*, 854, L2, doi: [10.3847/2041-8213/aaa9b2](https://doi.org/10.3847/2041-8213/aaa9b2)
- Maurin, D., Cheminet, A., Derome, L., Ghelfi, A., & Hubert, G. 2015, *Advances in Space Research*, 55, 363, doi: <https://doi.org/10.1016/j.asr.2014.06.021>

- McComas, D., Barraclough, B., Funsten, H., et al. 2000, *Journal of Geophysical Research: Space Physics*, 105, 10419, doi: [10.1029/1999ja000383](https://doi.org/10.1029/1999ja000383)
- Mordvinov, A. V., & Yazev, S. A. 2014, *Solar Physics*, 289, 1971, doi: [10.1007/s11207-013-0449-1](https://doi.org/10.1007/s11207-013-0449-1)
- Owens, M. J., & Forsyth, R. J. 2013, *Living Reviews in Solar Physics*, 10, 5, doi: [10.12942/lrsp-2013-5](https://doi.org/10.12942/lrsp-2013-5)
- Pishkalo, M. I. 2019, *Solar Physics*, doi: [10.1007/s11207-019-1520-9](https://doi.org/10.1007/s11207-019-1520-9)
- Potgieter, M. 1997, *Advances in Space Research*, 19, 883, doi: [https://doi.org/10.1016/S0273-1177\(97\)00297-4](https://doi.org/10.1016/S0273-1177(97)00297-4)
- . 2014a, *Advances in Space Research*, 53, 1415, doi: <https://doi.org/10.1016/j.asr.2013.04.015>
- Potgieter, M. S. 2013, *Living Reviews in Solar Physics*, 10, 3, doi: [10.12942/lrsp-2013-3](https://doi.org/10.12942/lrsp-2013-3)
- Potgieter, M. S. 2014b, *The Astrophysical Journal*, 785, 119, doi: [10.1088/0004-637X/785/2/119](https://doi.org/10.1088/0004-637X/785/2/119)
- Provornikova, E., Opher, M., Izmodenov, V. V., Richardson, J. D., & Toth, G. 2014, *ApJ*, 794, 29, doi: [10.1088/0004-637X/794/1/29](https://doi.org/10.1088/0004-637X/794/1/29)
- Putri, A. N. I., Herdiwijaya, D., & Hidayat, T. 2024, *Solar Physics*, 299, 12, doi: [10.1007/s11207-023-02249-9](https://doi.org/10.1007/s11207-023-02249-9)
- Scherrer, P., Wilcox, J., Svalgaard, L., et al. 1977, *Solar Physics*, 54, 353
- Smith, J., & Doe, J. 2022, *The Astrophysical Journal*, 926, 114, doi: [10.3847/1538-4357/ac4e19](https://doi.org/10.3847/1538-4357/ac4e19)
- Sun, X., Hoeksema, J. T., Liu, Y., & Zhao, J. 2015, *ApJ*, 798, 114, doi: [10.1088/0004-637X/798/2/114](https://doi.org/10.1088/0004-637X/798/2/114)
- Tomassetti, N. 2015, *Physical Review D*, 92, 081301, doi: [10.1103/PhysRevD.92.081301](https://doi.org/10.1103/PhysRevD.92.081301)
- Tomassetti, N., & Donato, F. 2015, *ApJL*, 803, L15, doi: [10.1088/2041-8205/803/2/L15](https://doi.org/10.1088/2041-8205/803/2/L15)
- Tomassetti, N., Orcinha, M., Barão, F., & Bertucci, B. 2017a, *The Astrophysical Journal Letters*, 849, L32, doi: [10.3847/2041-8213/aa9373](https://doi.org/10.3847/2041-8213/aa9373)
- Tomassetti, N., Orcinha, M., Barão, F., & Bertucci, B. 2017b, *The Astrophysical Journal Letters*, 849, L32, doi: [10.3847/2041-8213/aa9373](https://doi.org/10.3847/2041-8213/aa9373)
- Usoskin, I. G., Alanko-Huotari, K., Kovaltsov, G. A., & Mursula, K. 2005, *Journal of Geophysical Research (Space Physics)*, 110, A12108, doi: [10.1029/2005JA011250](https://doi.org/10.1029/2005JA011250)
- Webber, W. R. 2018, in *Cosmic Rays*, ed. Z. Szadkowski (Rijeka: IntechOpen), doi: [10.5772/intechopen.75877](https://doi.org/10.5772/intechopen.75877)
- Zerbo, J.-L., Amory-Mazaudier, C., & Ouattara, F. 2013, *Journal of Advanced Research*, 4, 265, doi: <https://doi.org/10.1016/j.jare.2012.08.010>

## APPENDIX

## A. ERROR ESTIMATION METHOD

To determine the weighted average and its uncertainty, we use the following formulas:

The weighted average of a set of measurements  $x_1, x_2, \dots, x_n$  with respective uncertainties  $\delta_1, \delta_2, \dots, \delta_n$  is given by:

$$x_{\text{avg}} = \frac{x_1 \cdot w_1 + x_2 \cdot w_2 + \dots + x_n \cdot w_n}{w_1 + w_2 + \dots + w_n} \quad (\text{A1})$$

Where the weight  $w_i$  is defined as:

$$w_i = \frac{1}{\delta_i^2} \quad (\text{A2})$$

The uncertainty on the weighted average  $\delta_{\text{avg}}$  is given by:

$$\delta_{\text{avg}} = \sqrt{\frac{1}{w_1 + w_2 + \dots + w_n}} \quad (\text{A3})$$

This method assigns more weight to measurements with smaller uncertainties and is commonly used in data analysis across various scientific fields. The standard error calculation ensures that measurements with higher precision contribute more significantly to the final result.

## B. SUPPLEMENTARY FIGURES

In Figure B1, by using Equation 2, we determined the minimum  $\chi^2/\text{ndf}$  value of 23.27/108, corresponding to an optimal weight of  $w = 0.78$ . This weight effectively smoothed the composite total solar magnetic field, eliminating fluctuations irrelevant to cosmic ray modulation. The significant reduction in chi-square values (around 6) indicates a clear improvement in the model's fit.

In Figure B2, we analyze the correlation between the weighted magnetic field strength and the electron flux in the rigidity range of 1-1.71 GV over the period from 2011 to 2014. We found a similar time delay of  $390_{-7}^{+56}$  days for electrons, consistent with the modulation effects observed for protons.

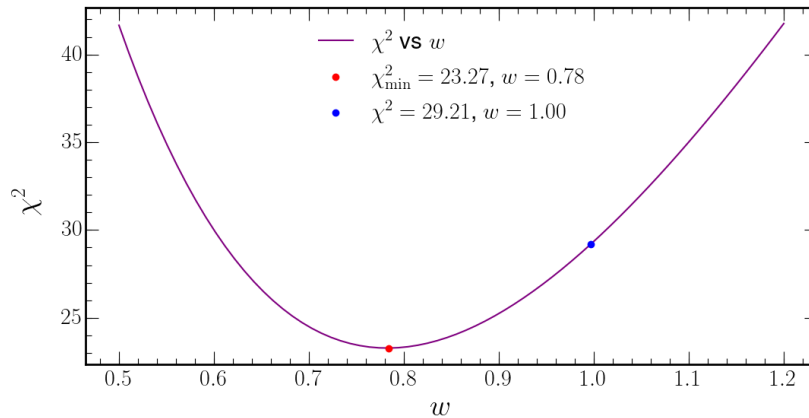


**Figure B1.**  $\chi^2$  distribution as a function of the effective weight of the magnetic fields. The red point shows the minimized  $\chi^2$ , while the blue point shows the  $\chi^2$  with  $w = 1.00$ , where the solar north and south magnetic fields have the same weight.



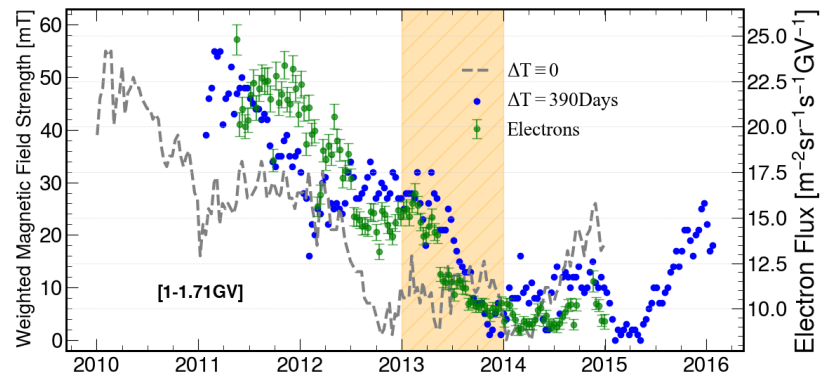


**Figure B2.** Comparison of weighted magnetic field strength and electron flux (1-1.71 GV) over Time: Magnetic field data is shown with no time shift (grey) and with a time shift of 390 days (blue), compared to electron flux measurements (green) from 2011 to 2014.